UNIVERSITY OF BATH

Link to publication

University of Bath

Surface-induced nonlinearity enhancement of TM modes in planar subwavelength waveguides

D. V. Skryabin,* A. V. Gorbach, and A. Marini

Centre for Photonics and Photonic Materials, Department of Physics, University of Bath, Bath BA2 7AY, UK
*Corresponding author: d.v.skryabin@bath.ac.uk

Using an asymptotic expansion of Maxwell equations and boundary conditions, we derive an amplitude equation for nonlinear TM modes in planar metal and dielectric waveguides. Our approach reveals that the physics of the significant enhancement of the nonlinear response in subwavelength waveguides with respect to their weakly guiding counterparts is hidden in surface effects. The corresponding enhancement factor is determined by the products of the surface discontinuities of the transverse field components and of the surface values of the longitudinal components of the electric field summed over all the interfaces. We present an insightful expression for the enhancement factor induced by the surface plasmon polaritons and discuss numerical and analytical results for the subwavelength dielectric and metal slot waveguides. Our theory also includes diffraction effects along the unbound direction in these waveguides.   © 2010 Optical Society of America

OCIS codes: 190.4390, 240.4350, 240.6680, 130.4310, 130.2790, 190.4350.

1. INTRODUCTION AND RATIONALE

Waveguiding on a subwavelength scale has become a practical reality with silicon slot waveguides providing a promising environment for nonlinear frequency conversion and ultrafast processing [1,2]. Metal and dielectric slot waveguides and surface plasmons are also actively researched for nonlinear applications and soliton effects; see, e.g., [3–9]. Submicrometer core optical fibers [10–12] have also been developed. The recent work carried out with the latter [12] has demonstrated that scaling of the nonlinear fiber parameter in the subwavelength geometry with the square of the projection of the Poynting vector on the propagation direction provides much better fit with the experimental measurements than the previous theories relying on the scaling with the $|\int_{-\infty}^{\infty} |\vec{\mathcal{E}}|^2 dS|^2$, where dS is the two-dimensional differential area in the plane perpendicular to the waveguide axis, and $\vec{\mathcal{E}}$ is the electric field. The older scaling can be traced back to the scalar wave equation [13], and its poor performance in the regime, when the guided mode strongly deviates from being a pure transverse wave, is not surprising.

Optical guidance at the planar metal surfaces and in planar dielectric slot waveguides intrinsically depends on the fact that TM modes have a nonzero longitudinal component of the electric field [4,5,7,8,14]. Nevertheless, existing theories deriving a nonlinear parameter of plasmonic waveguides either utilize the older scaling [4,7] suitable only for quasi-transverse fields or rely on cumbersome calculations [15] prohibiting qualitative understanding of the physical reasons inducing changes in the nonlinear response. Novel approaches developed for fibers and two-dimensional (2-D) silicon waveguides and giving the scaling of the nonlinear response with the projection of the Poynting vector utilize the modal expansion and reciprocity theorem [16–19]. The new scaling compares favorably with the experimental measurements [12], but still sheds little light on the physics of the significantly enhanced nonlinear response in subwavelength geometries [1,12].

To address this outstanding issue, we develop a rigorous and at the same time transparent asymptotic theory, which reveals that enhancement of the nonlinear response of TM modes in planar subwavelength waveguides happens exclusively due to surface effects. Namely, the enhancement factor is determined by the products of the surface discontinuities of the transverse field components and of the surface values of the longitudinal components of the electric field summed over all the interfaces. If either is disregarded, then no enhancement happens, and the results of the older theories are recovered. Thus, the longitudinal component of $\vec{\mathcal{E}}$ is important primarily through its surface value and not through its integrated average contribution.

2. ASYMPTOTIC EXPANSION FOR MAXWELL EQUATIONS AND BOUNDARY CONDITIONS

We consider a planar waveguide, where x is the direction perpendicular to the interfaces, z is the propagation direction, and y is the unbound direction, so that light can diffract along y. Evolution of the monochromatic field obeys time-independent Maxwell equations $\vec{\nabla} \times \vec{\nabla} \times \vec{\mathcal{E}} = \vec{\mathcal{D}}/\epsilon_0$ subject to boundary conditions at the interfaces. Here the electric field and displacement vectors are defined as $\frac{1}{2}\vec{\mathcal{E}} e^{-i\omega t} + \text{c.c.}$ and $\frac{1}{2}\vec{\mathcal{D}} e^{-i\omega t} + \text{c.c.}$, and ϵ_0 is the vacuum susceptibility. If $\epsilon(x)$ is the dielectric constant varying sharply at the interfaces, then $\vec{\mathcal{D}} = \epsilon_0(\epsilon\vec{\mathcal{E}} + \vec{\mathcal{N}})$, where $\vec{\mathcal{N}}$ is the nonlinear part of the displacement. The coordinates x, y, and z are normalized to the inverse wavenumber $k = 2\pi/\lambda$, where λ is the vacuum wavelength. We seek a solution corresponding to a nondegenerate guided mode in the form $\vec{\mathcal{E}} = \vec{E}(x,y,z)e^{i\beta z}$, where β is the propagation constant. We substitute $\vec{\mathcal{N}} = \vec{N}e^{i\beta z}$ and assume that $\epsilon = \epsilon_a + \epsilon_b$, where $\epsilon_a(x)$ is the leading term, and $\epsilon_b(x)$ is a possible correction, accounting, e.g., for linear absorption. Nonzero

components of the electric field of TM modes are E_x (perpendicular to the interfaces) and E_z (along the propagation direction). When diffraction along y direction is accounted for, the TM modes are transformed into quasi-TM ones, so that E_y is also nonzero but remains relatively small. Generic boundary conditions at the relevant interfaces are such that the tangential components of $\vec{E}$ and the normal components of the displacement $\epsilon\vec{E}+\vec{N}$ and all components of the magnetic field $\vec{H} = (\lambda c \epsilon_0/i2\pi)e^{-i\beta z}\vec{\nabla}\times\vec{E}e^{i\beta z}$ are continuous:

$$E_x:\ \Delta_j[\epsilon E_x + N_x] = 0, \qquad E_y:\ \Delta_j[E_y] = 0,$$
$$H_y:\ \Delta_j[\partial_x E_z - e^{-i\beta z}\partial_z(E_x e^{i\beta z})] = 0,$$
$$E_z:\ \Delta_j[E_z] = 0, \qquad H_z:\ \Delta_j[\partial_x E_y - \partial_y E_x] = 0, \qquad (1)$$

where the operator $\Delta_j[f]$ acting on a function $f(x)$ is defined as

$$\Delta_j[f] = \lim_{\delta\to 0}(f(x_j - \delta) - f(x_j + \delta)). \qquad (2)$$

Here x_j are the interface coordinates. Boundary conditions on H_x and H_z are not independent from the other ones and can be eliminated, but it is technically convenient to retain the H_z condition explicitly.

For a typical isotropic nonlinearity

$$\vec{N}(E_x, E_y, E_z) = \frac{1}{2}\chi_3\left(|\vec{E}|^2\vec{E} + \frac{1}{2}(\vec{E}\cdot\vec{E})\vec{E}^*\right), \qquad (3)$$

where χ_3 is the nonlinear susceptibility.

We assume that the exponential factor varies in z much faster than $\vec{E}$ itself, i.e., $|\partial_z\vec{E}| \ll \beta|\vec{E}|$. Further, it is assumed that the left-hand side of the above inequality, $\epsilon_b\vec{E}$, and $\vec{N}$ all have the same order of smallness $O(s^{3/2})$, where $s \ll 1$ is a dummy parameter. Also, $\epsilon_b \sim O(s)$, $\partial_z \sim O(s)$, $\sqrt{\chi_3}E_{x,z} \sim O(s^{1/2})$, $\sqrt{\chi_3}E_y \sim O(s)$, and $\partial_y \sim O(s^{1/2})$. For $\vec{E}$, we use the following ansatz:

$$E_x = A_x(\psi,x) + B_x(\psi,x) + O(s^{5/2}),$$
$$E_z = A_z(\psi,x) + B_z(\psi,x) + O(s^{5/2}),$$
$$E_y = C(\psi,x) + O(s^2), \qquad \psi = \psi(z,y), \qquad (4)$$

where $A_{x,z} \sim O(s^{1/2})$, $B_{x,z} \sim O(s^{3/2})$, and $C \sim O(s)$. All A, B and C do not depend on z and y explicitly, but only by means of the slowly varying function $\psi(z,y)$. Collecting all the $O(s^{1/2})$ terms, we find the following boundary value problem (BVP):

$$\hat{\mathcal{L}}\vec{A} = 0, \qquad E_x:\ \Delta_j[\epsilon_a A_x] = 0, \qquad E_z:\ \Delta_j[A_z] = 0, \qquad (5)$$

where

$$\vec{A} \equiv \begin{pmatrix} A_x \\ A_z \end{pmatrix}, \qquad \hat{\mathcal{L}} \equiv \begin{pmatrix} \beta^2 - \epsilon_a & i\beta\partial_x \\ i\beta\partial_x & -\partial_{xx}^2 - \epsilon_a \end{pmatrix}. \qquad (6)$$

For $\mathrm{Im}\epsilon_a = 0$, the BVP (5) is self-adjoint.

From possible solutions of this BVP, we select a nondegenerate bound mode $\vec{A} = I^{1/2}\psi(z,y)\vec{e}$, where

$$\vec{e}(x) = (e_x, e_z)^T \qquad (7)$$

is the mode profile, $\hat{\mathcal{L}}\vec{e} = 0$, and ψ is an undetermined function, $|\psi| \sim O(s^{1/2})$. Without any loss of generality, $\vec{e}$ can be assumed dimensionless, so that the field units are carried by

$I^{1/2}\psi$. The normalization factor I is chosen below in a way that $|\psi|^2$ is the power density (measured in watts per meter) carried in the z direction. Calculating the z component of the Poynting vector

$$P_z = \frac{1}{4k}\int_{-\infty}^{+\infty}(A_x H_y^* + A_x^* H_y)\mathrm{d}x = I|\psi|^2\frac{\epsilon_0 c}{2\beta k}Q, \qquad (8)$$

$$Q = \int_{-\infty}^{+\infty}\epsilon_a|e_x|^2\mathrm{d}x, \qquad (9)$$

where $H_y = \epsilon_a\epsilon_0 c/(\beta k)I^{1/2}\psi e_x$, we find $I = 2\beta k/(\epsilon_0 cQ)$. $|\psi|^2$ is measured in units of the power density and not of the power itself [13], since integration along the unbound direction y is not performed.

The BVP in the $O(s)$ order is

$$\partial_{xx}^2 C - (\beta^2 - \epsilon_a)C = 0, \qquad E_y:\ \Delta_j[C] = 0,$$
$$H_z:\ \Delta_j[\partial_x C] = I^{1/2}\partial_y\psi\Delta_j[e_x]. \qquad (10)$$

The right-hand side of the H_z boundary condition is nontrivial due to simultaneously nonzero diffraction and discontinuities of e_x; if either is disregarded, then $C = 0$. In general, $C = I^{1/2}e_y(x)\partial_y\psi(z,y)$, where $e_y(x)$ is bound ($\beta^2 > \lim_{|x|\to\infty}\epsilon_a$) and continuous in x and solves the above BVP with the H_z condition replaced by $\Delta_j[\partial_x e_y] = \Delta_j[e_x]$.

The BVP found in the $O(s^{3/2})$ order is

$$\hat{\mathcal{L}}\vec{B} = I^{1/2}\vec{J}, \qquad E_z:\ \Delta[B_z] = 0,$$
$$E_x:\ \Delta_j[\epsilon_a B_x] = -\Delta_j[\epsilon_b A_x] - I^{1/2}\psi|\psi|^2\Delta_j[n_x], \qquad (11)$$

where $\vec{B} = (B_x, B_z)^T$ and $\vec{J} = (J_x, J_z)^T$ is the displacement induced by the perturbations: $J_x = \partial_z\psi(2i\beta e_x - \partial_x e_z) + \partial_{yy}^2\psi (e_x - \partial_x e_y) + \psi\epsilon_b e_x + \psi|\psi|^2 n_x$, $J_z = -\partial_z\psi\partial_x e_x + \psi\epsilon_b e_z + \psi|\psi|^2 n_z$. For nonlinearity as in Eq. (3), we have $n_{x,z} \equiv IN_{x,z}(e_x, 0, e_z)$. Deriving an independent BVP for e_z and comparing it to the BVP for e_y, one can show that $e_z = i\beta e_y$. This identity couples the diffraction-induced e_y and the longitudinal field component and makes it possible to eliminate e_y from the following derivations.

3. NONLINEAR SCHRÖDINGER EQUATION AND SURFACE EFFECTS

Projecting Eq. (11) onto the linear TM mode, i.e., demanding $\int_{-\infty}^{\infty}(\vec{e}^*\cdot\hat{\mathcal{L}}\vec{B})\mathrm{d}x = I^{1/2}\int_{-\infty}^{\infty}(\vec{e}^*\cdot\vec{J})\mathrm{d}x$, we derive the amplitude equation for ψ and guarantee absence of secular terms in the solution for $\vec{B}$. An important aspect of the projection procedure is that we take $\int_{-\infty}^{\infty} = \int_{-\infty}^{x_1} + \sum_{j=1}^{N-1}\int_{x_j}^{x_{j+1}} + \int_{x_N}^{\infty}$, apply the integration by parts and use boundary conditions to evaluate the off-integral terms. Importantly, not only the right-hand side part of the projection condition, as in the perturbation theory with no midpoint boundaries, but also the left-hand one yields a nonzero outcome:

$$\int_{-\infty}^{\infty}(\vec{e}^*\cdot\hat{\mathcal{L}}\vec{B})\mathrm{d}x = -\eta PI^{1/2}(i\beta\partial_z\psi), \qquad (12)$$

$$\int_{-\infty}^{\infty}(\vec{e}^*\cdot\vec{J})\mathrm{d}x = i(2+\eta)\beta P\partial_z\psi + P(1+\eta)\partial_{yy}^2\psi + \psi\int_{-\infty}^{\infty}\epsilon_b|\vec{e}|^2\mathrm{d}x$$
$$+ \psi|\psi|^2\int_{-\infty}^{\infty}(e_x^* n_x + e_z^* n_z)\mathrm{d}x. \qquad (13)$$

Here

$$\eta = \frac{1}{\beta P}\sum_j (ie_z(x_j))^* \Delta_j[e_x], \qquad (14)$$

$$P = \int_{-\infty}^{\infty} |\vec{e}|^2 \mathrm{d}x. \qquad (15)$$

The resulting NLS equation for ψ is

$$i\frac{\partial \psi}{\partial(z/k)} + \frac{1}{2\beta k}\frac{\partial^2 \psi}{\partial(y/k)^2} + \alpha\psi + \Upsilon|\psi|^2\psi = 0, \qquad (16)$$

where the nonlinear parameter Υ can be expressed as

$$\Upsilon = g\gamma, \qquad (17)$$

$$\gamma = \frac{2k^2}{3\beta^2 P^2}\int_{-\infty}^{\infty}\epsilon_a n_2\left[|\vec{e}|^4 + \frac{1}{2}|\vec{e}^2|^2\right]\mathrm{d}x. \qquad (18)$$

Here we used $\chi_3 = (4/3)n_2\epsilon_0\epsilon_a c$, where n_2 is the Kerr coefficient. Parameter γ is defined to be similar to the one derived in the approaches dating back to the use of scalar wave equation [13], with equivalent expressions presented in [4,7]. Importantly, the nonlinear coefficient Υ differs from γ by the factor g:

$$g = \frac{1}{(1+\eta)^2}, \qquad (19)$$

which we call the *surface-induced nonlinearity enhancement factor*. The units of n_2 are m^2/W and the units of γ and Υ in our planar geometry are $1/\mathrm{W}$.

The enhancement factor g significantly deviates from $g = 1$, providing η significantly deviates from zero. The value of η [see Eq. (14)] is simultaneously determined by the longitudinal components of the field calculated exactly at the interfaces, $e_z(x_j)$, and by the jumps experienced by the transverse component, $\Delta_j[e_x]$. Using $\partial_x\epsilon_a e_x = -i\beta\epsilon_a e_z$ (div$_a\vec{\mathcal{E}} = 0$ condition for linear TM modes), we conclude that the phase of e_z can only be $\pm\pi/2$, and hence η is real. Calculating η for different metallic and dielectric waveguides (see Section 5 and Appendix A), we have found that $-1 < \eta < 0$. This implies $g > 1$ and hence field discontinuities at the surfaces and the surface values of the longitudinal field lead to the enhancement of the nonlinear response of the TM-guided modes.

The last and least important coefficient in Eq. (16) for our present purposes is

$$\alpha = \frac{k\sqrt{g}}{2P\beta}\int_{-\infty}^{\infty}\epsilon_b|\vec{e}|^2\mathrm{d}x. \qquad (20)$$

The physical meaning of α is determined by ϵ_b, which is the perturbation of the dielectric constant. $\alpha \sim \sqrt{g}$, and hence it is enhanced as well by the surface effects.

4. COMPARISON WITH PREVIOUS APPROACHES

In the weakly guiding limit of quasi-transverse modes $e_z \to 0$, $\beta^2 \to \epsilon_a$, and carrying n_2 through the integral, one finds $\gamma \simeq n_2 k/L_x$, where

$$L_x = \frac{\left(\int |e_x|^2 \mathrm{d}(x/k)\right)^2}{\int |e_x|^4 \mathrm{d}(x/k)} \qquad (21)$$

is the characteristic plasmon length along the x direction. The latter is the exact one-dimensional (1-D) analog of the γ given in [13].

Manipulating linear Maxwell equations and using the integration by parts, one can prove the auxiliary identity $g^{1/2}Q = \beta^2 P$ and show that $\Upsilon = \frac{2\beta^2 k^2}{3Q^2}\int_{-\infty}^{\infty}\epsilon_a n_2[|\vec{e}|^4 + \frac{1}{2}|\vec{e}^2|^2]\mathrm{d}x$. Notably, the latter expression does not contain g, which has been absorbed by Q. In its turn, $Q \sim P_z$, and thus our expression for Υ matches the nonlinear coefficients previously derived via the modal expansion and application of the reciprocity identity in, e.g., [16–19] for 2-D waveguides. Our results do not merely confirm the above ones for a particular case of TM modes in planar waveguides but reveal an insightful expression for the dimensionless factor g [see Eqs. (14) and (19)], making all the difference between the older and newer theories and thereby uncovering the pure surface origin of the nonlinearity enhancement. Applications of the reciprocity-based approach in quasi-1-D geometry, when not only nonlinearity but also diffraction should be considered as a perturbation, remain unknown to us, and therefore direct comparison is not possible. The propagation operator in Eq. (16) is $i\partial_z + \frac{1}{2\beta k}\partial^2_{yy}$, with the diffraction coefficient $1/(2\beta k)$ (βk is the physical propagation constant). Note that, in some other theories treating diffraction of surface TM waves (see, e.g., [7]), the propagation operator contains additional coefficients making the diffraction rate different from $1/(2\beta k)$. In this respect, the linear part of our results is analogous to [20].

5. SURFACE-INDUCED NONLINEARITY ENHANCEMENT IN BASIC WAVEGUIDE GEOMETRIES

To evaluate the surface-induced nonlinearity enhancement factor g, we have considered several basic waveguide geometries [see Figs. 1(d)–1(f)]. While below we discuss numerical [as shown in Figs. 1(a)–1(c)] and simplest analytical results for g, we also present the analytical field profiles and expressions for η used to calculate g in Appendix A.

First is the waveguide of width w (dielectric constant ϵ_w) embedded into the cladding material with dielectric constant $\epsilon_d < \epsilon_w$[see Figs. 1(a) and 1(d)]. Let us remind that all the distances are scaled to $2\pi/\lambda$. We find that, in this case, g tends to 1 in both limits $w \to \infty$ and $w \to 0$ and has a well-pronounced maximum for the waveguide width of the order of wavelength $w \sim 1$, thus implying resonant nonlinear response of the dielectric waveguides [see Fig. 1(a)]. In a very realistic case of silicon surrounded by air, g rises to $\simeq 4$.

Placing two identical dielectric waveguides close together creates the guidance of the symmetric ($e_x(x) = e_x(-x)$) TM mode inside the low-index slot [see Figs. 1(b) and 1(e)]. Changing the slot width d, we found that g tends to the corresponding values for the single waveguides of width w and $2w$ in the corresponding limits $d \to \infty$ and $d \to 0$. Location of the maximum of g also varies with w, but most typically is found for practically accessible $d \simeq 0.1$ [see Fig. 1(b)]. Figure 2(a) shows a comparison of γ and Υ calculated as the function of the slot width. To express γ and Υ in the units of $1/\mathrm{W/m}$, familiar for slot waveguides with a 2-D cross section (see, e.g.,

in [1]), we divided them by $L_y = 100$ nm, which is the characteristic length scale along the y coordinate. We have chosen n_2 to be the same inside the slot and in dielectric stripe to illustrate the pure geometrical impact on the nonlinearity enhancement.

The other slot waveguide we are considering consists of the two metal ($\epsilon_m < 0$) interfaces separated by the slot of width d filled with the dielectric ($\epsilon_d > 0$) [see Fig. 1(f)]. For $d \gg 1$, we deal with almost independent surface plasmon polaritons (SPPs) at every interface. In this case, g can be calculated in an elegant form (while in the other cases the dispersion law for β remains unresolved explicitly; see Appendix A for details):

$$g_{\text{spp}} = \frac{(\epsilon_d^2 + \epsilon_m^2)^2}{(\epsilon_d + \epsilon_m)^4} \qquad (22)$$

and is clearly far from 1. g_{spp} tends to infinity very rapidly when the contrast parameter $\epsilon_d/|\epsilon_m|$ tends to 1 (plasmon resonance), which is the cutoff condition for SPPs to exist at the single interface. In this limit, both phase and group velocity of the plasmon become zero, so that new orders of smallness have to be introduced in our asymptotic procedure, which is likely to result in the amplitude equation different from the one derived above. Nonlinear parameter Υ for a plasmon also can be calculated explicitly (see Appendix A) and is given by

$$\Upsilon_{\text{spp}} = \frac{2k^2 \epsilon_d n_2}{3} \frac{\epsilon_m^2}{(\epsilon_d + \epsilon_m)^2} \left[1 + \frac{1}{2} \left(\frac{\epsilon_m + \epsilon_d}{\epsilon_d - \epsilon_m} \right)^2 \right]. \qquad (23)$$

Note, that the divergence of Υ_{spp} for $\epsilon_d/|\epsilon_m| \to 1$ is weaker than the one of g_{spp}.
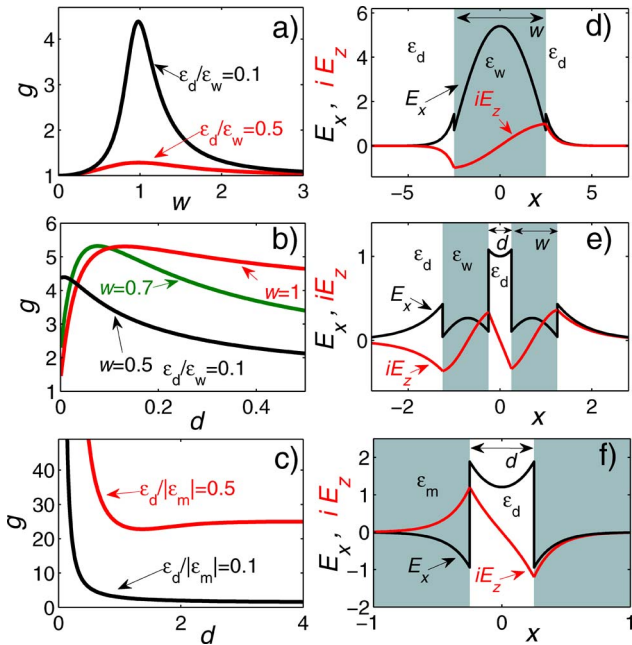

Fig. 1. (Color online) (a)–(c) Surface-induced nonlinearity enhancement factor g for three different waveguide geometries. The corresponding waveguides and electric field profiles are shown in (d)–(f). (a), (d) Single dielectric waveguide of the width w. (b), (e) Dielectric slot waveguide, i.e., two dielectric waveguides separated by the slot width d. (c), (f) Metal slot waveguide, i.e., two metal interfaces separated by the slot width d. All other notations and features are explained in the text.
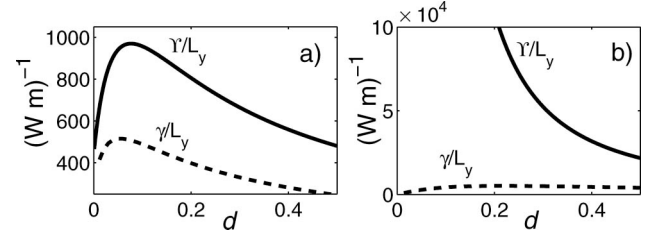

Fig. 2. Comparison between γ/L_y (dashed curves) and the surface-enhanced Υ/L_y (solid curves) nonlinear parameters for the (a) silicon and (b) metal slot waveguides with the polymer-filled slot. n_2 for silicon and polymer are assumed to be the same $4 \cdot 10^{-18}$ m^2/W, while the dielectric constants are $\epsilon_w = 12$ and $\epsilon_d = 3.2$, respectively. $w = 0.7$, $\lambda = 1.5$ μm, and $L_y = 100$ nm. In (b), the metal is assumed linear and $\epsilon_m = -25$, $\epsilon_d = 4$, $\lambda = 0.8$ μm.

In the metal slot waveguides, the surface enhancement g is easily getting very significant; even for moderate contrast $\epsilon_d/|\epsilon_m| = 0.1$–$0.5$ we have $g \simeq 20$–50, while close to the plasmon resonance it shoots to the infinity. Note that, in the metal slot waveguides, the enhancement factor rises sharply as the slot width tends to zero ($g \sim 1/d^2$, as can be derived using η given in Appendix A), while in the dielectric slot g drops after reaching the maximum for some small d [cf. Figs. 1(a) and 1(c)]. Behavior of the nonlinear parameters Υ and γ is also different. In the dielectric slot, Υ and γ remain bound for $d \to 0$ and $d \to \infty$ [see Fig. 2(a)]. However, in the metal slot $\lim_{d\to 0}\gamma = 0$, while $\lim_{d\to 0}\Upsilon = \infty$ [see Fig. 2(b)]. Thus, in the narrow metal slots, the surface enhancement makes not only quantitative but also qualitative impact on nonlinear response.

6. SUMMARY AND CONCLUSIONS

In summary, using a new asymptotic approach, which rigorously treats boundary conditions, we have derived a nonlinear amplitude equation for TM modes in planar optical waveguides. Our approach has enabled us to introduce and analyze the surface-induced nonlinearity enhancement factor g. This dimensionless factor attains values between 1 and 10 in dielectric slot waveguides and shoots up toward infinity for surface plasmons and in metallic subwavelength slots. The g factor provides a clear link between the traditional results for the nonlinear parameter in the weakly guiding regime [13] and the recent calculations and experimental measurements done for subwavelength structures [16–18]. More than this, it shows that the nonlinearity enhancement in the subwavelength regime is attributed to the surface values of the longitudinal component of the electric field and to the interface jumps of the transverse component. For material constants and waveguide geometries leading to the divergent g factors, a new asymptotic theory should be developed, which will be reported elsewhere. Though it still needs to be proved formally, one can expect that, for the 2-D TM (or quasi-TM) modes, the expression for g [see Eqs. (14) and (19)] should contain a contour integral along the waveguide boundaries instead of the sum over all the interfaces. Mentioning quasi-TE modes, the significant surface effects are unlikely, due to continuity of the leading order electric field component across the interface and smallness of the longitudinal field.

APPENDIX A

Below we present analytical expressions for the field profiles and parameter η determining the enhancement factor g [see

Eq. (19)] for the waveguides described in Section 4. We, however, have chosen to omit the rather cumbersome equations for the dielectric slot waveguide as the one shown in Fig. 1(e) and whose field structure has been reported in [14].

1. Dielectric Waveguide as in Fig. 1(d)

The TM mode of this waveguide is

$$
e_x \begin{cases} \frac{i\beta}{\kappa}\cos(\kappa x) & |x| < w/2, \\ \frac{i\beta}{q}\sin(\kappa w/2)e^{-q(|x|-w/2)} & |x| > w/2, \end{cases} \tag{A1}
$$

$$
e_z = \begin{cases} \sin(\kappa x) & |x| < w/2, \\ \frac{x}{|x|}\sin(\kappa w/2)e^{-q(|x|-w/2)} & |x| > w/2, \end{cases} \tag{A2}
$$

where $\kappa^2 = \epsilon_w - \beta^2$, $q^2 = \beta^2 - \epsilon_d$, and β is defined from $\epsilon_d\kappa\tan(\kappa w/2) = \epsilon_w q$. Then, we obtain

$$
\eta = -2\left(\frac{\epsilon_w}{\epsilon_d} - 1\right)
$$
$$
\times \left[\frac{\beta^2}{\kappa^2} - 1 + w\kappa\left(\frac{\beta^2}{\kappa^2} + 1\right)\sin^{-1}(\kappa w) + \frac{\epsilon_w}{\epsilon_d}\left(\frac{\beta^2}{q^2} + 1\right)\right]^{-1}. \tag{A3}
$$

$\eta < 0$ and $\eta \to 0$ in both limits $w \to \infty (\kappa \to 0)$ and $w \to 0 (q \to 0)$, and hence there is an optimal waveguide width maximizing the surface enhancement [see Fig. 1(a)].

2. Surface Plasmon at a Metal–Dielectric Interface

Field of the surface plasmon is given by

$$
e_x = i\beta\left[\frac{1}{q_d}e^{-q_d x}\theta(x) - \frac{1}{q_m}e^{q_m x}\theta(-x)\right], \tag{A4}
$$

$$
e_z = e^{-q_d x}\theta(x) + e^{q_m x}\theta(-x), \tag{A5}
$$

where $\theta(x)$ is the Heaviside function, $q_{d,m} = \sqrt{\beta^2 - \epsilon_{d,m}}$, and $\beta^2 = \epsilon_m\epsilon_d/(\epsilon_m + \epsilon_d)$. Here d and m stand for dielectric and metal, respectively. Then, we obtain

$$
\eta = -\frac{2\epsilon_d/|\epsilon_m|}{1 + \epsilon_d^2/\epsilon_m^2}, \tag{A6}
$$

which is used to derive Eq. (22). An explicit form of γ for plasmons is

$$
\gamma = \frac{2k^2\epsilon_d n_2}{3}\frac{(1 - \epsilon_d/|\epsilon_m|)^2\left[1 + \frac{1}{2}\left(\frac{1-\epsilon_d/|\epsilon_m|}{1+\epsilon_d/|\epsilon_m|}\right)^2\right]}{[1 + \epsilon_d^2/\epsilon_m^2]^2}. \tag{A7}
$$

Thus, γ tends to zero as $\epsilon_d/|\epsilon_m| \to 1$, but at a rate weaker than the corresponding enhancement factor g_{spp} [see Eq. (22)] tends to infinity, thereby yielding $\Upsilon \to \infty$ [see Eq. (23)].

3. Metal Slot Waveguide as in Fig. 1(f)

The metal slot mode with symmetry $e_x(x) = e_x(-x)$ and $e_z(x) = -e_z(-x)$ is given by

$$
e_x = \begin{cases} -\frac{i\beta}{q_d}\cosh(q_d x) & |x| < d/2, \\ \frac{i\beta}{q_m}\sinh(q_d d/2)e^{-q_m(|x|-d/2)} & |x| > d/2, \end{cases} \tag{A8}
$$

$$
e_z = \begin{cases} \sinh(q_d x) & |x| < d/2, \\ \frac{x}{|x|}\sinh(q_d d/2)e^{-q_m(|x|-d/2)} & |x| > d/2, \end{cases} \tag{A9}
$$

where $q_{d,m}$ are as above, and β is found from $|\epsilon_m|q_d\tanh(q_d d/2) = \epsilon_d q_m$. η in this case is given by

$$
\eta = -2\left(1 - \frac{\epsilon_d}{\epsilon_m}\right)
$$
$$
\times \left[\frac{\beta^2}{q_d^2} + 1 + dq_d\left(\frac{\beta^2}{q_d^2} - 1\right)\sinh^{-1}(q_d d) - \frac{\epsilon_d}{\epsilon_m}\left(\frac{\beta^2}{q_m^2} + 1\right)\right]^{-1}. \tag{A10}
$$

REFERENCES

1. C. Koos, P. Vorreau, T. Vallaitis, P. Dumon, W. Bogaerts, R. Baets, B. Esembeson, I. Biaggio, T. Michinobu, F. Diederich, W. Freude, and J. Leuthold, "All-optical high-speed signal processing with silicon-organic hybrid slot waveguides," Nat. Photon. **3**, 216–219 (2009).
2. A. Di Falco, L. O'Faolain, and T. F. Krauss, "Dispersion control and slow light in slotted photonic crystal waveguides," Appl. Phys. Lett. **92**, 083501 (2008).
3. D. Mihalache, G. I. Stegeman, C. T. Seaton, E. M. Wright, R. Zanoni, A. D. Boardman, and T. Twardowski, "Exact dispersion relations for transverse magnetic polarized guided waves at a nonlinear interface," Opt. Lett. **12**, 187–189 (1987).
4. E. Feigenbaum and M. Orenstein, "Plasmon-soliton," Opt. Lett. **32**, 674–676 (2007).
5. A. R. Davoyan, I. V. Shadrivov, and Y. S. Kivshar, "Nonlinear plasmonic slot waveguides," Opt. Express **16**, 21209–21214 (2008).
6. G. A. Wurtz and A. V. Zayats, "Nonlinear surface plasmon polaritonic crystals," Laser Photon. Rev. **2**, 125–135 (2008).
7. A. R. Davoyan, I. V. Shadrivov, and Y. S. Kivshar, "Self-focusing and spatial plasmon-polariton solitons," Opt. Express **17**, 21732–21737 (2009).
8. A. V. Gorbach and D. V. Skryabin, "Spatial solitons in periodic nanostructures," Phys. Rev. A **79**, 053812 (2009).
9. K. F. MacDonald, Z. L. Samson, M. I. Stockman, and N. I. Zheludev, "Ultrafast active plasmonics," Nat. Photon. **3**, 55–58 (2009).
10. L. M. Tong, R. R. Gattass, J. B. Ashcom, S. L. He, J. Y. Lou, M. Y. Shen, I. Maxwell, and E. Mazur, "Subwavelength-diameter silica wires for low-loss optical wave guiding," Nature **426**, 816–819 (2003).
11. G. S. Wiederhecker, C. M. B. Cordeiro, F. Couny, F. Benabid, S. A. Maier, J. C. Knight, C. H. B. Cruz, and H. L. Fragnito, "Field enhancement within an optical fibre with a subwavelength air core," Nat. Photon. **1**, 115–118 (2007).
12. S. Afshar V., W. Q. Zhang, H. Ebendorff-Heidepriem, and T. M. Monro, "Small core optical waveguides are more nonlinear than expected: experimental confirmation," Opt. Lett. **34**, 3577–3579 (2009).
13. G. P. Agrawal, *Nonlinear Fiber Optics* (Academic, 2001).
14. V. R. Almeida, Q. F. Xu, C. A. Barrios, and M. Lipson, "Guiding and confining light in void nanostructure," Opt. Lett. **29**, 1209–1211 (2004).
15. A. Marini and D. V. Skryabin, "Ginzburg–Landau equation bound to the metal–dielectric interface and transverse nonlinear optics with amplified plasmon polaritons," Phys. Rev. A **81**, 033850 (2010).

16. C. Koos, L. Jacome, C. Poulton, J. Leuthold, and W. Freude, "Nonlinear silicon-on-insulator waveguides for all-optical signal processing," Opt. Express **15**, 5976–5990 (2007).
17. S. Afshar V. and T. M. Monro, "A full vectorial model for pulse propagation in emerging waveguides with subwavelength structures part I: Kerr nonlinearity," Opt. Express **17**, 2298–2318 (2009).
18. R. M. J. Osgood, N. C. Panoiu, J. I. Dadap, X. Liu, X. Chen, I. Hsieh, E. Dulkeith, W. M. Green, and Y. A. Vlasov, "Engineering nonlinearities in nanoscale optical systems: physics and applications in dispersion-engineered silicon nanophotonic wires," Adv. Opt. Photon. **1**, 162–235 (2009).
19. B. A. Daniel and G. P. Agrawal, "Vectorial nonlinear propagation in silicon nanowire waveguides: polarization effects," J. Opt. Soc. Am. B **27**, 956–965 (2010).
20. G. D. Valle and S. Longhi, "Geometric potential for plasmon polaritons on curved surfaces," J. Phys. B **43**, 051002 (2010).